

# RETRIEVAL OF 3-D WATER VAPOR FIELD USING A NETWORK OF SCANNING COMPACT MICROWAVE RADIOMETERS

Sharmila Padmanabhan<sup>1</sup>, Steven C. Reising<sup>1</sup> and Jothiram Vivekanandan<sup>2</sup>

<sup>1</sup>Department of Electrical and Computer Engineering  
Colorado State University  
Fort Collins, CO 80523-1373

<sup>2</sup>National Center for Atmospheric Research  
Boulder, CO 80301

## ABSTRACT

Quantitative precipitation forecasting is currently limited by the paucity of observations of thermodynamic variables in the troposphere, including water vapor. Specifically, measurements of 3-D water vapor fields are needed at sub-meso- $\gamma$  scales in pre-storm conditions. This can be achieved using a network of remote sensors to retrieve the water vapor field with high spatial and temporal resolution. Such measurements may be used for assimilation into and validation of numerical weather prediction (NWP) models. Conventional measurements of water vapor density profiles are obtained using *in-situ* probes on-board weather balloons, including radiosondes. Remote sensing techniques to retrieve moisture profiles include ground-based networks receiving Global Navigation Satellite Systems (GNSS) signals, including GPS, and GPS receivers aboard the COSMIC satellite constellation for atmospheric occultation. These methods provide measurements with high vertical resolution but with coarse horizontal resolution. Differential Absorption Lidars (DIAL) can retrieve water vapor with comparable resolution to that of radiosonde observations [1]. However, these lidars are expensive, and their operation is limited to clear-sky conditions due to the high opacity of clouds at optical wavelengths.

Inversion of brightness temperatures measured by upward-looking, ground-based microwave radiometers allows the estimation of vertical profiles with high temporal resolution in both clear and cloudy conditions. However, assimilation of retrieved 3-D water vapor fields with improved spatial coverage into NWP models in pre-storm conditions has the potential for substantial impact on numerical weather prediction of convective storm activity. Measurements using a network of multi-frequency microwave radiometers can provide the necessary information to retrieve the 3-D distribution of water vapor in the troposphere.

**Index Terms**— radiometer, water vapor, precipitation, tomography

## 1. INTRODUCTION

Water vapor in the troposphere is highly variable, both temporally and spatially. Profiles of water vapor are typically measured with high vertical resolution using radiosondes. However, in the U.S., radiosondes are launched from National Weather Service stations separated by  $\sim 70$  km on average. Radiosondes are not reusable,

restricting operational launches to twice daily, 0 and 12 UTC, at most stations. Improvements in quantitative precipitation forecasting continue to pose substantial scientific challenges [2], including the location and amount of precipitation, as well as understanding the underlying processes and mechanisms of convective initiation [3]. Currently, water vapor profiling by commercial radiometers is limited to zenith-pointing observations [4].

Despite their importance to quantitative precipitation forecasting, current observational technologies for measuring water vapor are inadequate, in part because water vapor content varies over three orders of magnitude on fine spatial and temporal scales in the troposphere. Table I provides characteristics of currently available water vapor measurements from remote and *in-situ* sensors. COSMIC (Constellation Observing System for Meteorology, Ionosphere and Climate)/FormoSat moisture products using the GPS radio occultation technique have high vertical resolution on the order of 100–500 m [5]. However, the horizontal resolution of the retrieved moisture profiles is coarse, i.e.  $\sim 200$  km. The prediction of convective initiation requires the knowledge of water vapor content on meso- $\gamma$  scales (2-5 km) [6]. Scanning measurements using a network of multi-frequency microwave radiometers observing overlapping volumes have the potential to provide improved horizontal and temporal resolution. Tomographic inversion and spatial interpolation techniques will be implemented to retrieve the 3-D structure of the water vapor in the troposphere with fine spatial and temporal resolution. To this end, compact microwave radiometers designed for network deployment were developed and fabricated at the Microwave Systems Laboratory at Colorado State University (CSU) [7].

## 2. COMPACT MICROWAVE RADIOMETER FOR HUMIDITY PROFILING (CMR-H)

To obtain high-resolution measurements of humidity in the troposphere, the Microwave Systems Laboratory at CSU has developed, fabricated, tested and deployed two Compact Microwave Radiometers for Humidity Profiling (CMR-H). The CMR-H takes advantage of the latest monolithic microwave integrated circuit (MMIC) technology and packaging developed by the communications industry to achieve small size (24 cm x 18 cm x 16 cm / 9" x 7" x 6"), low mass (6 kg / 13 lbs.) and low power

consumption (25-50 W, depending on the season of the year). In addition, the low cost of CMR-H facilitates its deployment in a network. Table II provides the specifications of CMR-H.

CMR-H field measurements were validated at the NCAR Mesa Laboratory during the Refractivity Experiment For H<sub>2</sub>O Research and Collaborative operational Technology Transfer (REFRACTT'06). The observational focus of REFRACTT'06 was to obtain very high resolution measurements of water vapor variability and transport in the convective boundary layer using a wide variety of instruments. The CMR-H performed collocated measurements with the commercially-available Radiometrics WVP-1500. Water vapor profiles retrieved from CMR-H and WVP-1500 brightness temperatures were compared with Vaisala RS-92 radiosonde measurements. During REFRACTT'06, Vaisala RS-92 radiosondes were launched from the same location as CMR-H for measurement comparison [8].

On Oct. 9, 2007, we deployed two CMR-H's, spaced 6 km apart, and launched a Vaisala RS-92 radiosonde from one of the radiometer locations at Christman Field, Fort Collins, CO. Figure 1 shows good agreement between water vapor profiles measured by RS-92 radiosonde and those retrieved from the brightness temperatures measured by the two zenith pointing CMR-H's. The integrated precipitable water vapor values of the two profiles agree to within 10 %.

Since the water vapor inversion problem is ill-posed and non-linear, the Bayesian optimal estimation technique [9-10] was used to invert the brightness temperatures measured at 22.12, 22.67, 23.25 and 24.50 GHz to obtain vertical water vapor profiles. The inversion used the nearest-in-time radiosonde observation (RAOB) performed at the Denver/Stapleton, CO weather station as the *a-priori* water vapor profile. The water vapor density at the surface was corrected using an NWS station measurement.

TABLE I. CURRENTLY AVAILABLE MEASUREMENTS OF WATER VAPOR

Sensor	Horizontal Resolution (km)	Vertical Resolution (km)	Temporal Resolution (hr)	Frequency Band
Radiosonde	~70 km	0.05-0.1	12	<i>In-situ</i> sensor
GPS Ground Networks	20-50	0.5-1 (expected)	30 min	L-band
COSMIC	200-400	0.1-0.5	15 min (1-hr lag)	L-band
AMSU-B	20	2	12	183 GHz
GOES	50	2	1	Infrared

TABLE II. COMPACT MICROWAVE RADIOMETER SPECIFICATIONS

Parameter	CSU Compact Microwave Radiometer for Humidity Profiling (CMR-H)
Frequency Channels (GHz)	22.12, 22.67, 23.25 and 24.50
Sensitivity (K) @ 1-sec int.	0.2 - 0.3
3-dB Antenna Beamwidth (°)	3.0 - 4.0
Calibration	Internal: Noise Diode and Reference Load External: Tipping curve, Microwave absorber at ambient temperature and LN <sub>2</sub>
Mass	6 kg
Dimensions	24 cm x 18 cm x 16 cm
DC Power Consumption	50 W

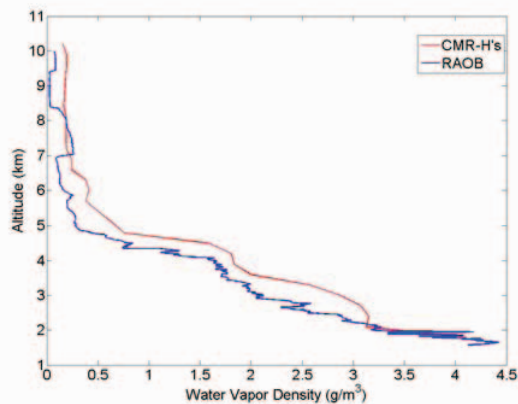


Figure 1. Comparison of water vapor density profiles measured by radiosonde and retrieved from CMR-H measurements.

For ground-based deployment, brightness temperature measurements from a coordinated sensor network in which each “node” is a CMR-H can be used to retrieve 3-D images of humidity in the network’s coverage region, as described in Section 3. CMR-H, mounted atop a pan-tilt positioner, is capable of scanning at a rate of 7°/sec in elevation and 25°/sec in azimuth.

### 3. 3-D WATER VAPOR RETRIEVAL METHODOLOGY

An Observation System Simulation Experiment (OSSE) was performed to demonstrate the retrieval of the 3-D distribution of water vapor in the troposphere using measurements from a network of scanning microwave radiometers. For the OSSE, the 3-D water vapor distribution predicted by the Weather Research and Forecasting (WRF) numerical weather prediction model was compared with retrievals from synthetic brightness temperatures measured by a network of CMR-H's. The WRF model output simulated a cold front and deep convection over northwest Indiana (40.7° N, 86° W) from 1:00 UT to 3:00 UT with 500-m spatial resolution.

A forward radiative transfer model [9-10] uses the high-resolution WRF model output to calculate synthetic brightness temperatures at the CMR-H frequencies as a function of both azimuth and elevation angles. To determine an optimal scanning strategy, the decorrelation time of the atmosphere was estimated by finding the peak of the autocorrelation of a long time series (~3000 s) of zenith microwave brightness temperatures measured during REFRACTT'06. The decorrelation time of the atmospheric downwelling emission *on the spatial scales of the radiometer measurement* was determined to be on the order of tens of minutes for an unstable atmosphere in the presence of rapidly evolving moisture gradients. This provides an upper bound, or maximum duration during which a radiometer node must complete a scan of its coverage volume, typically the upper hemisphere centered at the node. If each radiometer node completes its hemispherical scan within this duration, all measurements can be considered to be simultaneous, again given the spatial scales of the measurement.

An optimally-packed topology for a radiometer network with three CMR-H's is shown in Figure 2, assuming 10 km between each pair of nearest-neighbor nodes. The proposed volumetric scanning of each CMR-H radiometer node is every 30° in azimuth

(12 angles) and 8 angles in elevation from zenith to 30° above the horizon. The elevation angles were chosen based on an eigenvalue analysis of the ray length in each grid cell. The segments in Figure 2 represent the azimuthal angles for each radiometer in the network within a triangular “unit cell” of the network.

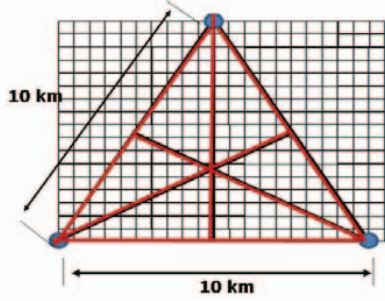


Figure 2. Locations and azimuthal scan directions for 3 CMR-H network nodes

To retrieve water vapor profiles between nodes as well as above each node, algebraic tomographic reconstruction was used to combine brightness temperatures observed by multiple radiometers in overlapping scan volumes. The scanning technique described above is similar to a transform-based fanbeam projection method used in medical imaging [11]. This is based on the simultaneous requirements to measure a large number of projections and for these projections to be uniformly distributed over 180° or 360°. However, brightness temperature measurements by a radiometer network do not satisfy both of these requirements simultaneously. As opposed to medical imaging, reconstruction problems of this type tend to be more amenable to solution by algebraic matrix inversion reconstruction techniques, such as those used in seismic tomographic retrievals.

A forward radiative transfer model uses measured water vapor (WRF model outputs for the OSSE) to calculate the brightness temperature that would be measured by a radiometer as

$$T_B(z) = T_{CMB} e^{-\tau(0,z)} + \int_0^z k_{abs}(z') T(z') e^{-\tau(z',z)} dz' \quad (1)$$

where  $T_B$  is the brightness temperature in K,  $z$  is the height above ground level in km,  $k_{abs}$  is the absorption coefficient in Np/km,  $\tau$  is the optical depth and  $T_{CMB}$  is the cosmic microwave background radiation (2.73 K). If the scanned domain is divided into  $M$  grid cells, the forward model can be expressed as [12]

$$T_{Bi} = T_{CMB} e^{-\sum_{j=1}^M k_{abs\_j} \Delta r_{ij}} + \sum_{j=1}^M k_{abs\_j} T_j e^{-\tau_{ij}} \Delta r_{ij} \quad (2)$$

where  $T_{Bi}$  is the integrated brightness temperature measured by a radiometer pointing at the  $i^{\text{th}}$  elevation angle;  $k_{abs\_j}$  is the absorption coefficient in the  $j^{\text{th}}$  grid cell;  $T_j$  is the thermodynamic temperature in the  $j^{\text{th}}$  grid cell;  $\Delta r_{ij}$  is the length of the ray of the  $i^{\text{th}}$  elevation angle within the  $j^{\text{th}}$  grid cell; and the opacity  $\tau_{ij}$  is given as

$$\tau_{ij} = \sum_{l=1}^{j-1} k_{abs\_j} \Delta r_{il} \quad (3)$$

Replacing the exponential terms in (2) with a truncated Taylor series, the linearized forward model becomes

$$T_{Bi} = T_{CMB} \left( 1 - \sum_{j=1}^M k_{abs\_j} \Delta r_{ij} \right) + \sum_{j=1}^M k_{abs\_j} T_j \left( 1 - \sum_{l=1}^{j-1} k_{abs\_j} \Delta r_{il} \right) \Delta r_{ij} \quad (4)$$

Next, we start with a reference profile of the pressure, temperature and water vapor density for a typical atmosphere for the general latitude, longitude and season. For example, the mid-latitude summer reference atmospheric profile is used in this study. The absorption coefficient in each grid cell is calculated at the CMR-H frequencies using the most up-to-date microwave absorption models of the atmosphere [13-14]. Variations in the absorption coefficient from the reference value can be related to variations in the calculated brightness temperature from the reference value,  $T_{Brefi}$ , also found using the forward model with the reference profile as input. The two quantities are related by a Jacobian matrix  $G$  as

$$T_{Bi} - T_{Brefi} = G \cdot (k_{abs\_j} - k_{absref\_j}) \quad (5)$$

The Jacobian matrix elements are given as

$$g_{ij} = \frac{\partial(\Delta T_{Bi})}{\partial(\Delta k_j)} \quad (6)$$

where  $g_{ij}$  is the partial derivative of the change in the brightness temperature at the  $i^{\text{th}}$  elevation angle with respect to the change in absorption coefficient in the  $j^{\text{th}}$  grid cell. The variation in the absorption coefficient for a measured variation in brightness temperature can be computed as

$$\Delta K = G^{-1} \Delta T_{Bi} \quad (7)$$

However, finding the value of  $G$  is an underdetermined problem, so there is no unique solution. Regularization techniques are needed to solve such ill-posed problems. Therefore, Bayesian optimal estimation was used to calculate the values of  $\Delta K$ . The Kalman filter technique [9] was implemented to take into account the sequential time evolution of water vapor densities, meeting the requirement that the retrieved values vary smoothly between successive measurements in time. In such cases, the previous measurement provides prior information about the water vapor density at the current time, provided that the evolution of the water vapor density in time can be modeled. The general formulation of the Kalman filter is as follows:

$$\Delta k_{abs\_at} = M_t (\Delta k_{abs(t-1)}) \quad (8)$$

$$M_t = \frac{\partial M_t (\Delta k_{abs(t-1)})}{\partial \Delta k_{abs\_at}} \quad (9)$$

$$\Delta k_{abs(t)} = \Delta k_{abs\_at} + S_{\Delta k_{abs,at}} G_t^T (G_t S_{\Delta k_{abs,at}} G_t^T + S_{T_B})^{-1} \bullet [\Delta T_B - G \Delta k_{abs\_at}] \quad (10)$$

where  $M_t$  is the model evolution parameter, used sequentially in time. At time  $t-1$ , an estimate of  $\Delta k_{abs(t-1)}$  is made, with an error covariance  $S_{\Delta k_{abs(t-1)}}$ . The stochastic prediction equation (8) is used to construct a prior estimate  $\Delta k_{abs\_at}$  and its covariance  $S_{\Delta k_{abs,at}}$  at time  $t$ . This estimate is used in Bayesian optimal estimation to calculate a water vapor density estimate at time  $t$ . The Jacobian  $G$  has elements as in (6). The absorption coefficients retrieved in each high-resolution WRF model grid cell (0.5 km x 0.5 km typical horizontal resolution) at the four operating frequencies of CMR-H were used to compute the water vapor density in the grid cell using the Van-Vleck Weisskopf absorption line shape, which varies with altitude due to pressure broadening [15]. 3-D moisture fields were retrieved and compared with the WRF model output. Figure 3(a) shows the WRF model output of the water vapor density at 3.4 km AGL at 3:00 UT. Figure 3(b) shows the percentage error in the retrieval at 3:00 UT obtained by algebraic tomographic reconstruction, as described above. The *a-priori* used

for this retrieval was the WRF model output at 2:00 UT. Water vapor densities at the unsampled locations were estimated by using the kriging spatial interpolation technique. The kriging algorithm was based on the spatial characteristics of water vapor densities, including semi-variogram and correlation lengths, calculated using the high-resolution WRF model output [16-17]. The OSSE results show that the 3-D water vapor density field can be retrieved with an accuracy of better than 15-20% at all altitudes above ground level.

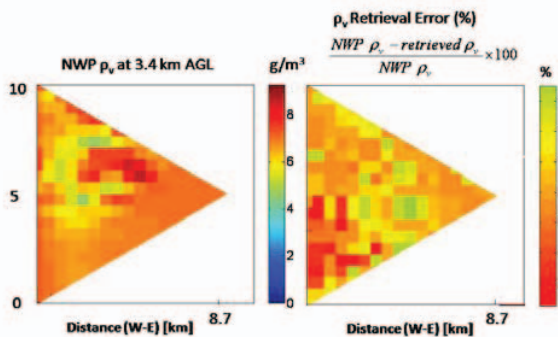


Figure 3. (a) WRF model output of the water vapor density at 3.4 km above ground level (AGL) over northwest Indiana at 3:00 UT. (b) Percentage error of the water vapor density retrieved from synthetic brightness temperature measurements also at 3.4 km AGL with WRF model output at 2:00 UT used as the *a priori*.

#### 4. SUMMARY

The Compact Microwave Radiometer for Humidity Profiling (CMR-H) is small, light-weight, inexpensive, robust and consumes little power. The low cost of CMR-H enables the deployment of a sufficient number of scanning microwave radiometers to form a network. CMR-H was designed for network operation, in which each sensor, or network "node," performs a complete volumetric scan within a few minutes. Radiometer measurements of the same volume from multiple perspectives, i.e. different sensor nodes, will be combined using tomographic inversion to retrieve the 3-D water vapor field as a function of time. An OSSE was performed to demonstrate the retrieval of the 3-D water vapor field and compared with WRF model output with a grid resolution of 0.5 km. The OSSE demonstrated a retrieval accuracy of 15-20%.

Water vapor profiles retrieved from the brightness temperatures measured by two CMR-H's show good agreement with those measured by RS-92 radiosondes. Two CMR-H's have been field demonstrated and a third is being fabricated. In order to obtain high spatial and temporal resolution water vapor fields for validation of NWP models, we will deploy a ground-based test network of three radiometers during upcoming experiments, in collaboration with radiosonde measurements and GPS networks.

#### 5. ACKNOWLEDGMENT

This material is based on work supported by the National Science Foundation under Grant No. ATM-0456270 to Colorado State University and Grant No. ATM-0239722 to the University of Massachusetts Amherst. as well as by the Advanced Study Program at the National Center for Atmospheric Research.

#### 6. REFERENCES

- [1] J. L. Machol and co-authors, "Preliminary measurements with an automated compact differential absorption lidar for the profiling of water vapor," *Appl. Opt.*, vol. 43, no. 15, pp. 3110-3121, 2004.
- [2] K. A. Emanuel and co-authors, "Report of the first prospectus development team of the US weather research program to NOAA and the NSF," *Bull. Amer. Meteorol. Soc.*, vol. 76, pp. 1194-1208, 1995.
- [3] A. Hense, A. Gerd, C. S. Kottmeier, C. Simmer and V. Wulfmeyer, "Quantitative Precipitation Forecast," [www.meteo.unibonn.de/projekte/SPPMeteo/reports/SPPLeitAntrag\_English.pdf], 2003.
- [4] D. Cimini, T. J. Hewison, L. Martin, J. Guldner, C. Gaffard and F. S. Marzano, "Temperature and humidity profile retrievals from ground-based microwave radiometers during TUC," *Meteorol. Z.*, vol. 15, no. 5, pp. 1-12, Feb. 2006.
- [5] G. Beyerle, T. Schmidt, J. Wickert, S. Heise, M. Rothacher, G. Konig-Langlo, and K. B. Lauritse, "Observational and simulations of receiver-induced refractivity biases in GPS radio occultation," *J. Geophys. Res.-Atmos.*, vol. 109, D01106, doi: 10.1029/2005JD006673, 2004.
- [6] M. N. Deeter and K. F. Evans, "Mesoscale variations of water vapor inferred from millimeter-wave imaging radiometer during TOGA COARE," *Journal of Applied Meteorology, Notes and Correspondence*, vol. 36, 183-188, Feb. 1997.
- [7] F. Iturbide-Sanchez, S. C. Reising and S. Padmanabhan, "A miniaturized spectrometer radiometer based on MMIC technology for tropospheric water vapor profiling," *IEEE Trans. Geosci. Remote Sensing*, vol. 44, no. 7, pp. 2181-2193, Jul. 2007.
- [8] S. Padmanabhan, J. Vivekanandan, S. C. Reising and F. Iturbide-Sanchez, "Estimation of 3-D water vapor distribution using a network of Compact Microwave Radiometers", in *Proc. IGARSS, Barcelona, Spain, Jul. 2007*, pp. 251-254.
- [9] C. D. Rodgers, *Inverse Methods for Atmospheric Sounding: Theory and Practice*, World Scientific Publishing Co. Ltd., 2000.
- [10] T. J. Hewison and C. Gaffard, "1D-VAR retrieval of temperature and humidity profiles from ground-based microwave radiometers," *Proc. IEEE MicroRad'06*, San Juan, Puerto Rico, Mar. 2006, pp. 235-240.
- [11] A. C. Kak and M. Slaney, *Principles of Computerized Tomographic Imaging*, IEEE Press, 1988.
- [12] A. V. Bosisio and G. Drufulca "Retrieval of two-dimensional absorption coefficient structure from a scanning radiometer at 23.8 GHz," *Radio Sci.*, vol. 38, no. 3, 8038, doi:10.1029/2002RS002628, 2003.
- [13] P. W. Rosenkranz, Erratum: "Water vapor microwave continuum absorption: A comparison of measurements and models", *Radio Sci.*, vol. 34, no. 4, p. 1025, Jul.-Aug. 1999.
- [14] J. C. Liljegren, S.-A. Boukabara, K. Cady-Pereira, and S. A. Clough, "The effect of the half-width of the 22-GHz water vapor line on retrievals of temperature and water vapor profiles with a 12-channel microwave radiometer," *IEEE Trans. Geosci. Remote Sens.*, vol. 43, no. 5, pp. 1102-1108, May 2005.
- [15] P. W. Rosenkranz, "Absorption of microwaves by atmospheric gases," Chapter 2 in Michael A. Janssen (ed.), *Atmospheric Remote Sensing by Microwave Radiometry*, M. A. Janssen, Ed., New York, J. Wiley & Sons, Inc., 1994, pp. 37-90.
- [16] R. Webster and M. Oliver, *Geostatistics for Environmental Scientists*, John Wiley, 2003.
- [17] A. Jindal and K. Psounis, "Modeling spatially correlated data in sensor networks," *ACM Trans. Sensor Networks*, vol. 2, no. 4, pp. 466-499, Nov. 2006.